Electron–LO-phonon scattering rates in semiconductor quantum wells

S. Rudin
Electronics Technology and Devices Laboratory, U.S. Army Laboratory Command, Fort Monmouth, New Jersey 07703-5000

T. L. Reinecke
Naval Research Laboratory, Washington D.C. 20375-5000
(Received 10 October 1989)

We calculate scattering rates for an electron interacting with polar optical phonons in a semiconductor quantum well based on a microscopic lattice-dynamics approach for the phonons. We employ an analytic approximation to lattice-dynamics results given by Huang and Zhu for quantum-well phonons. The resulting electron relaxation rates are compared with the rates obtained by employing "slab" and "guided" phonon modes which were used in previous studies. The intrasubband and intersubband electron relaxation rates are given as functions of quantum-well width, and the relative contributions of the confined and the interface modes are discussed for the three different phonon models.

I. INTRODUCTION

In recent years there has been considerable interest in the effects of electron-phonon scattering and electron relaxation in $GaAs/Al_xGa_{1-x}As$ multiple-quantum-well structures. The corresponding electron scattering rates have been studied experimentally by time-resolved Raman scattering[1,2] and infrared spectroscopy.[3] The results suggest that the electron intersubband relaxation rate is dominated by their interaction with LO phonons (if the subband separation exceeds the LO-phonon energy) or by their interactions with LA phonons (otherwise).

It has been pointed out[4,5] that the effects of the confinement of the phonons should be taken into account in order to obtain a realistic estimate for the electron-phonon scattering and the electron relaxation rates. The quantum-well structure causes there to be "bulklike" phonon modes confined to the well layer and also gives rise to "interface" modes. Phonon confinement affects relaxation rates mainly through changes in the selection rules for transitions involving subband electrons and through changes in the magnitudes of the interaction.

Electron–LO-phonon interactions in quantum-well systems have been studied using two different macroscopic approaches to the confined phonons. One corresponds to the "slab modes" of a free ionic slab[6,7] and the other to the "guided modes"[5,8] of a layered structure. These models differ in the way the boundary conditions are placed on the electrostatic potential or vibrational amplitude of the phonons. The question of the physically correct boundary conditions cannot be determined within a macroscopic model but must be approached within microscopic lattice dynamics. Recently a simple microscopic model[9,10] has been advanced for the phonon modes of a superlattice, and analytic approximations for the results of this microscopic model have been given.[9,10]

In the present work we calculate the intersubband and intrasubband relaxation rates based on this analytic approximation to the microscopic model. We also give the relaxation rates corresponding to the two macroscopic models and compare the results with those based on the microscopic model. It is the intent of the present work to provide a formalism for electron relaxation rates based on a microscopic description of the confined phonons and to discuss the regimes of validity of macroscopic models. By comparing such results to experiment it is then possible to see quantitatively what effects are due to the confined phonons and when other physical effects are necessary to describe the experimental situation.

For definiteness numerical results are given for a model GaAs/GaAlAs system, which is of considerable experimental interest. The formalism is applicable to other semiconductor quantum-well systems.

II. CONFINED PHONONS

In studies of the electron–LO-phonon interaction in semiconductor quantum wells the confined phonon modes are usually approximated by either slab modes[6,7] or guided modes[5,8] which are solutions of a macroscopic dielectric model with different boundary conditions. These solutions are extensively reviewed by Klein[11] and by Cardona.[12]

The slab modes are obtained using boundary conditions on electric field without regard to the atomic displacements at the interface. We call this model 1. In this model the electric potential has nodes at the interface, and the vibrational amplitudes are given by[6]

$$U_{n+} \propto \sin(n\pi z/L), \quad n=1,3,5,\ldots \tag{1}$$

$$U_{n-} \propto \cos(n\pi z/L), \quad n=2,4,6,\ldots \tag{2}$$

where L is the width of the quantum well centered at $z=0$.

This approximation for the confined modes is acceptable only if the in-plane component of the polarization is

much larger than its z component; this condition can be written in terms of the phonon wave vector[11] as $q \gg \pi/L$ where $\mathbf{q}=(q_x,q_y)$.

In the opposite limit, $q \ll \pi/L$, electric boundary conditions are neglected in favor of the approximate boundary condition on the atomic displacements at the interface.[12] We call this model 2. The vibrational amplitudes of the confined modes, called "guided modes" by Ridley,[5] are given by[8,12]

$$U_{n+} \propto \cos(n\pi z/L), \quad n=1,3,5,\ldots \tag{3}$$

$$U_{n-} \propto \sin(n\pi z/L), \quad n=2,4,6,\ldots . \tag{4}$$

These modes were employed by Ridley[5] recently to calculate the intrasubband and intersubband electron transition rates in a quantum well.

The in-plane component q of the phonon wave vector in general can be comparable to π/L; e.g., for a GaAs quantum well of width $L=150$ Å we obtain for the transition from the bottom of the subband 2 to the subband 1 $qL \sim 3$. In such a case neither of the two approximations (models 1 and 2) is applicable.

In order to obtain analytic results for scattering rates, an alternative to the dielectric model solutions would be some simple analytical approximation for the numerical solutions of some microscopic model for the superlattice phonons. There exist in the literature a number of the microscopic model calculations for the bulklike confined modes. Here we employ the relatively simple model of Huang and Zhu[9,10] which we call model 3. This model gives modes for which both electric potential and polarization have nodes at the interfaces. Huang and Zhu have suggested simple analytic approximations for the numerical solutions.[10] This allows us to derive the electron–polar-phonon interaction matrix element in a simple form.[10] We have recently employed this model in the exciton linewidth calculations.[13]

In the Huang-Zhu model, the optical vibrations between oppositely charged ions are given by a simple-cubic lattice of charged oscillators. A superlattice of length $2ma$ is imposed on this system with lattice constant a. The two materials that form a superlattice differ only in their bulk LO and TO frequencies. The resulting dynamical matrix is then diagonalized numerically.[9]

The electric potential inside one layer is given by

$$V(\mathbf{r},z) \propto \Phi_n(z)\exp(i\mathbf{q}\cdot\mathbf{r}) , \tag{5}$$

where $\mathbf{q}$ and $\mathbf{r}$ are two-dimensional (2D) vectors.

Huang and Zhu proposed the following analytical approximations for the numerical solutions of this microscopic model: for odd modes,

$$\Phi_{n+}=\sin(\mu_n\pi z/L)+C_n z/L, \quad n=3,5,7,\ldots \tag{6}$$

for even modes,

$$\Phi_{n-}=\cos(\mu_n\pi z/L)-(-1)^{n/2}, \quad n=2,4,6,\ldots \tag{7}$$

where μ_n are successive solutions of the equation

$$\tan(\mu\pi/2)=\mu\pi/2 \tag{8}$$

with the smallest one (μ_1) omitted, and C_n are given by

$$C=-2\sin(\mu\pi/2) . \tag{9}$$

These approximations to the microscopic model solutions are also exact solutions of the dielectric model which incorporates boundary conditions both on potentials and displacements.[10] For the few first modes the functions given by Eqs. (6) and (7) are approximately orthogonal for $qL/\pi \lesssim 1$. These modes, however, contribute most to the scattering rate, and we use Eqs. (6) and (7) as analytical approximations for the confined phonon modes. The odd modes in Eq. (6) start from $n=3$. The $n=1$ mode is absent because the corresponding bulk mode becomes an interface mode.[10]

III. ELECTRON-PHONON INTERACTION

The electron-phonon interaction Hamiltonian derived from Fröhlich interaction[7,18,10] is given by

$$H_{e\text{-}p}=\lambda V^{-1/2}\sum_{q,n}\sum_{\alpha=\pm}\exp(i\mathbf{q}\cdot\mathbf{r})t_n(q)u_{n\alpha}(z) \times[a_{n\alpha}(\mathbf{q})+a^{\dagger}_{n\alpha}(-\mathbf{q})] \tag{10}$$

where $a, a^{\dagger}$ are phonon operators; and λ is given by

$$\lambda^2=4\pi e^2\hbar\omega_{\mathrm{LO}}(\epsilon_{\infty}^{-1}-\epsilon_0^{-1}) . \tag{11}$$

ϵ_0, ϵ_{∞} are, respectively, the static and high-frequency dielectric constants for GaAs, ω_{LO} is the GaAs LO-phonon frequency, and $-e$ is the electron charge.

In models 1 and 2

$$t_n(q)=(q^2+\pi^2n^2/L^2)^{-1/2} . \tag{12}$$

In model 3 we have $t_n(q)=(2I_n)^{-1/2}$ where I_n is defined as

$$I_n=\frac{1}{L}\int_{-L/2}^{L/2}dz\left[q^2\Phi_n^2+\left[\frac{d\Phi_n}{dz}\right]^2\right] \tag{13}$$

with Φ_n given by Eqs. (6) and (7). $u_{n\alpha}(z)$ is defined as follows: in model 1

$$\begin{aligned} u_{n+}&=\cos(\pi nz/L), \quad n=1,3,5,\ldots \\ u_{n-}&=\sin(\pi nz/L), \quad n=2,4,6,\ldots ; \end{aligned} \tag{14}$$

in model 2

$$\begin{aligned} u_{n+}&=\sin(\pi nz/L), \quad n=1,3,5,\ldots \\ u_{n-}&=\cos(\pi nz/L), \quad n=2,4,6,\ldots ; \end{aligned} \tag{15}$$

in model 3 u are given by Eqs. (6) and (7): $u_{n\alpha}=\Phi_{n\alpha}$.

IV. SCATTERING RATES FOR ELECTRONS INTERACTING WITH CONFINED PHONONS

For model 2 the scattering rate was calculated by Ridley.[5] Here we proceed similarly in the evaluation of the rate for model 3. Considering one-phonon processes only, the scattering rate is obtained from the following equation:[5]

$$W(k)=(2\pi/\hbar)\int dN_f\,\delta(E-E')|\langle \mathbf{k}'|H_{e\text{-}p}|\mathbf{k}\rangle|^2 \tag{16a}$$

$$=(\lambda^2/2\pi L\hbar)\sum_n \int d^2q\, t^2(q)|G_n|^2 \times\delta\left[\frac{\hbar^2k^2}{2m}-\frac{\hbar^2k'^2}{2m}\pm\hbar\omega_{\rm LO}\right] \times(N_{\rm LO}+\tfrac{1}{2}\mp\tfrac{1}{2})\delta_{\mathbf{k},\,\mathbf{k}'\mp\mathbf{q}}\ , \tag{16b}$$

where $N_{\rm LO}$ is the LO-phonon occupation number; the upper sign is for phonon absorption, and the lower is for emission. G_n is given by

$$G_n=\int_{-L/2}^{L/2}dz\,\psi'(z)u_n(z)\psi(z) \tag{17}$$

where ψ,ψ' are the electron envelope subband wave functions in the initial and final states, respectively.

We assume here the usual effective-mass approximation for the conduction band. To simplify calculations we also assume an infinite barrier height for the electron thus neglecting electron tunneling into the barrier. Then for the two lowest subbands

$$\psi_1(z)=(2/L)^{1/2}\cos(\pi z/L)\Theta(L/2-z)\ ,$$

$$E_1=\pi^2\hbar^2/2mL^2 \tag{18}$$

$$\psi_2(z)=(2/L)^{1/2}\sin(2\pi z/L)\Theta(L/2-z),\quad E_2=4E_1 \tag{19}$$

where m is an effective mass for the conduction band.

We then obtain, for the intraband $(1\rightarrow1)$ case, for model 1,

$$G_{n+}^{(11)}=-2(-1)^{(n+1)/2}\left[\frac{1}{\pi n}+\frac{\pi n}{(2\pi)^2-(\pi n)^2}\right],\quad n=1,3,\ldots \tag{20}$$

$$G_{n-}^{(1,1)}=0,\quad n=2,4,\ldots\ ;$$

model 2,

$$G_{n+}^{(11)}=0\ ,\qquad G_{n-}^{(11)}=\tfrac{1}{2}\delta_{n,2}\ ; \tag{21}$$

model 3,

$$G_{n+}^{(11)}=0\ ,\qquad G_{n-}^{(11)}=\tfrac{3}{2}\delta_{n,2}-(-1)^{n/2}(1-\delta_{n,2})\ . \tag{22}$$

After performing the q integration in Eq. (16) we obtain for the intraband transition rate the following expression:

$$W_{11}(k)=(s\lambda^2m/\hbar^3L)\sum_{n\alpha}|G_{n\alpha}^{(11)}|^2(N_{\rm LO}+\tfrac{1}{2}\mp\tfrac{1}{2}) \times[Q_1^4+\chi_n^4+2\chi_n^2(2k^2\pm Q_1^2)]^{-1/2} \tag{23}$$

where

$$Q_1^2=2m\omega_{\rm LO}/\hbar\ . \tag{24}$$

In models 1 and 2

$$\chi_n=\pi n/L,\quad s=1\ ; \tag{25}$$

in model 3

$$\chi_n=\pi n/L\sqrt{3},\quad s=\tfrac{1}{3}\ . \tag{26}$$

For model 2 Eq. (23) is identical to one obtained by Ridley in Ref. 5.

For the interband $2\rightarrow1$ transition we obtain, for model 1,

$$G_{n+}^{(21)}=0\ ,\qquad G_{n-}^{(21)}=(2/\pi)n(-1)^{n/2}[1/(n^2-9)-1/(n^2-1)]\ ; \tag{27}$$

for model 2,

$$G_{n+}^{(12)}=\tfrac{1}{2}(\delta_{n,1}+\delta_{n,2})\ ,\qquad G_{n-}^{(12)}=0\ ; \tag{28}$$

and for model 3,

$$G_n^{(12)}=16C_n/9\pi^2+(2\mu_n/\pi)\cos(\mu_n\pi/2)\times[1/(\mu_n^2-1)-1/(\mu_n^2-9)]\ ,\quad n=3,5,\ldots$$
$$G_{n-}^{(12)}=0,\quad n=2,4,\ldots\ . \tag{29}$$

In the evaluation of the scattering rate W_{21} we assume that $E_2-E_1>\hbar\omega_{\rm LO}$. We then obtain

$$W_{21}(k)=(\lambda^2m/\hbar^3L)\sum_{n\alpha}A_n^{-1}|G_{n\alpha}^{(21)}|^2(N_{\rm LO}+\tfrac{1}{2}\mp\tfrac{1}{2}) \times[Q_\pm^4+B_n^2/A_n^2+2(B_n/A_n)(2k^2+Q_\pm^2)]^{-1/2} \tag{30}$$

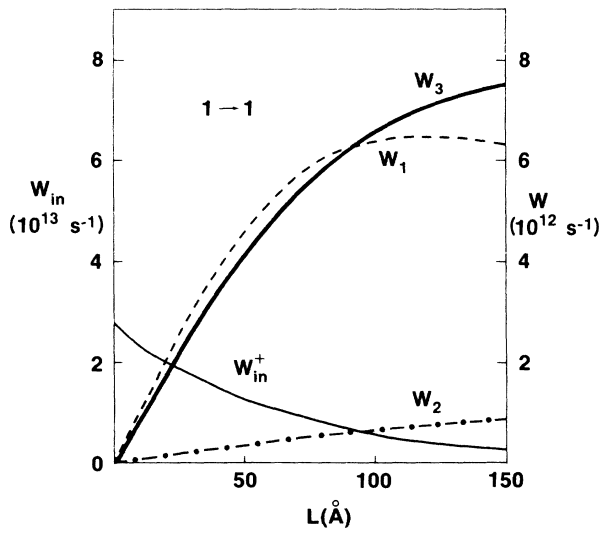

FIG. 1. Intrasubband $1\rightarrow1$ scattering rates in GaAs quantum wells. The rate of the electron transition with emission of one phonon is related to the quantity W plotted here through $W_{11}=(N_{\rm LO}+1)W$. W_1, W_2, and W_3 show contribution of confined phonon modes to W (right axis) using three different models considered in the text: (1) slab modes, (2) guided modes, and (3) Huang-Zhu model. The contribution of the interface phonon modes $W_{\rm in}^+$ is also shown here (left axis).

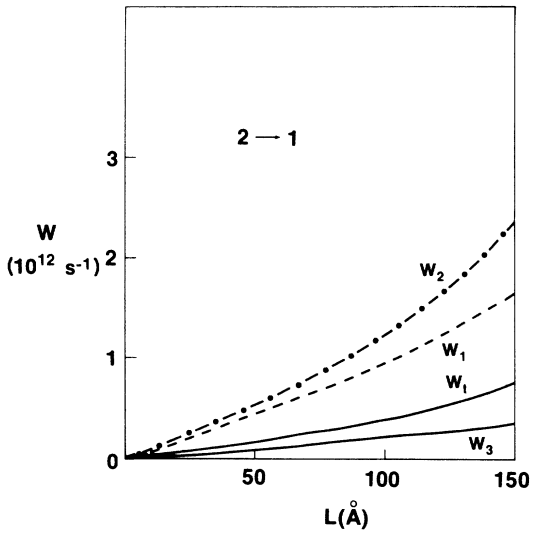

FIG. 2. Intersubband 2→1 scattering rates in GaAs quantum wells. The rate of the electron transition with emission of one phonon is related to the quantity W plotted here through $W_{21}=(N_{\rm LO}+1)W$. W_1, W_2, and W_3 show the contributions of confined phonon modes to W in the three different models as in Fig. 1. The contribution of the interface modes is comparable to W_3, and the total rate in the Huang-Zhu model, $W_t=W_3+W_{\rm in}$, is shown here.

where

$$Q_{\pm}^2=(2m/\hbar^2)(E_2-E_1\pm\hbar\omega_{\rm LO}) . \tag{31}$$

In models 1 and 2

$$A_n=1,\quad B_n=\chi_n^2=\pi^2n^2/L^2,\quad n=1,3,5,\ldots . \tag{32}$$

In model 3

$$A_n=1+C_n^2(\tfrac{1}{6}-1/\mu^2\pi^2),\quad B_n=\mu_n^2\pi^2/L^2 ,\quad n=3,5,\ldots . \tag{33}$$

Using Eqs. (8) and (9) we can rewrite G_n in model 3 as

$$G_n^{(12)}=(2C/\pi^2)[\tfrac{8}{9}-1/(\mu^2-1)+1/(\mu^2-9)] . \tag{34}$$

We now consider the phonon emission part of the intraband rate $W_{11}(k)$ at $k=Q_1$, so that the electron energy is just enough to emit one LO phonon. In model 1 all odd n modes contribute to W, in model 2 only the $n=2$ mode contributes, and in model 3 all even n modes ($n=2,4,\ldots$) contribute. The results are given in Fig. 1 for $W=W_{11}(Q_1)/(N_{\rm LO}+1)$.

For the interband transition 2→1 we consider the transition rate at $k=0$ so that the electron is initially at the bottom of the second subband. In model 1 all even n modes contribute, in model 2 only $n=1$ and $n=3$ modes contribute, and in model 3 modes with odd n starting with $n=3$ contribute to W_{21}. The results are given in Fig. 2 for $W=W_{21}(0)/(N_{\rm LO}+1)$.

V. CONTRIBUTION OF THE INTERFACE MODES TO THE ELECTRON SCATTERING RATE

In the preceding sections we discussed the contribution of the confined phonon modes. In the evaluation of the total transition rates, however, the interface phonon modes[14,15] can be at least as important as the confined modes. The classification of phonons as confined and interface modes is valid only in a dielectric continuum model. In the microscopic model there is a certain amount of mode mixing.[10] However, it has been shown[16] that in some respects the interface modes obtained from the continuum model give a reasonably good representation of these modes. To simplify the discussion and avoid summation over the minizone we shall use the interface modes obtained for the double heterostructure[14] rather than those for the superlattice.[15]

The dielectric model has two symmetric and two antisymmetric solutions. The interaction Hamiltonian is given by[14]

$$H_\alpha=\sum_{q,\mu}\left[\frac{2\pi e^2 f_{\alpha\mu}}{\hbar A q\omega_{\alpha\mu}}\right]^{1/2}\exp(i\mathbf{q}\cdot\mathbf{r})\exp(-qL/2)\times[\exp(qz)\pm\exp(-qz)](1\pm\gamma)^{-1/2}\times[a_{\alpha\mu}(\mathbf{q})+a_{\alpha\mu}^{\dagger}(-\mathbf{q})] . \tag{35}$$

The index $\alpha=s,a$ denotes the parity with respect to the z axes; the index $\mu=\pm$ distinguishes between the two solutions of given parity. The quantities that enter Eq. (35) are defined as follows:

$$\gamma=\exp(-qL) , \tag{36}$$

$$f_{\alpha\mu}=\left|\frac{\hbar^2(\omega_{\alpha\mu}^2-\omega_{\rm TO1}^2)(\omega_{\alpha\mu}^2-\omega_{\rm TO2}^2)}{(\omega_{\alpha+}^2-\omega_{\alpha-}^2)(\epsilon_{1\alpha}+\epsilon_{2\alpha})}\right| , \tag{37}$$

$$\epsilon_{1s}=\epsilon_{1\infty}(1-\gamma),\quad \epsilon_{2s}=\epsilon_{2\infty}(1+\gamma) ,\quad \epsilon_{1a}=\epsilon_{1\infty}(1+\gamma),\quad \epsilon_{2a}=\epsilon_{2\infty}(1-\gamma) . \tag{38}$$

$\omega_{\rm TO1}$, $\omega_{\rm TO2}$ are the bulk TO-phonon frequencies, assumed here to be dispersionless. Index 1 refers to the well material (GaAs); index 2 refers to the barrier material. The expression for $\omega_{\alpha\mu}$ can be found in Ref. 14. Because the dispersion of the $\omega_{\alpha\mu}(q)$ turns out to be rather small we shall ignore it in the calculation of the electron transition rates and use the asymptotic values for large qL (reached at $qL\sim3$). The scattering rates are then evaluated from Eqs. (16a) and (35).

These rates are energy dependent, and the results are shown in Figs. 1 and 2 for $W_{11}(Q_1)$ and $W_{21}(0)$ where Q_1 is given in Eq. (24). For the intraband transition 1→1 only the symmetric ($\alpha=s$) modes contribute, and $W_{\rm in}$ is dominated by the higher-energy mode $\mu=+$. This quantity labeled $W_{\rm in}^{+}$ is shown in Fig. 1. In models 3 and 1 it becomes comparable with the contribution of the confined modes to W_{11} at $L\approx100$ Å and dominates the scattering rate at $L<70$ Å. In model 2 it is actually the dominant contribution to W_{11} at all values of L that are shown in Fig. 1. In models 1 and 2 the interband 2→1 rate is dominated by the contribution of the confined

phonons for all quantum-well widths. In model 3 the contribution of the interface modes to the interband $2\rightarrow 1$ rate is comparable to the contribution of the confined modes to W, and we show in Fig. 2 the total rate $W_t(2\rightarrow 1)$ defined as $W_3+W_{\rm in}$.

The following parameter values were used in Figs. 1 and 2 for the GaAs/AlAs system: $m=0.0665$, $\hbar\omega_{\rm LO1}=36.8$ meV, $\hbar\omega_{\rm LO2}=47.7$ meV, $\hbar\omega_{\rm TO1}=34$ meV, $\hbar\omega_{\rm TO2}=44$ meV, $\epsilon_{1\infty}=10.48$, $\epsilon_{2\infty}=8.16$, $\epsilon_{10}=12.35$, and $\epsilon_{20}=10$.

VI. DISCUSSION

In the present work we have given a treatment of the scattering of electrons by confined LO phonons and of the phonon-induced relaxation times of electrons based on a microscopic treatment of the phonons. This treatment uses an analytic approximation to lattice dynamics of a simple microscopic model. We have also given results for two macroscopic models of the confined phonons and have discussed the regimes of validity of these models. The macroscopic models use "slab modes" (model 1) and "guided modes" (model 2). We have pointed out that for the purpose of calculating the relaxation rates, the phonon wave vectors are typically $qL/\pi\sim 1$, and thus the approximations used in the two macroscopic models are not justified. The analytic representation of the microscopic model discussed here (model 3) is more appropriate.

The results for the intrasubband relaxation rates in Fig. 1 indicate that those for models 1 and 3 are similar, and that for model 2 is considerably smaller. The reason for the smaller value in model 2 is that only one confined phonon mode contributes as a result of selection rules. For the intersubband $(2\rightarrow 1)$ relaxation rates, on the other hand, the rate for model 3 is considerably smaller than those for models 1 and 2. The small value for model 3 results from the absence of the lowest confined mode which has become the interface mode. Thus we see that neither model 1 nor 2 provides a good approximation for the intersubband relaxation rate given by model 3. Several experimental results giving information about intersubband relaxation rates in quantum-well structures have been reported recently.[1-3] Time-resolved Raman scattering experiments of Tatham *et al.*[1] have given an estimate for the upper bound on the intersubband relaxation time of 1 psec for a GaAs quantum well of width 146 Å at 30 K. These authors have noted that the results of both the slab mode and guided mode phonon models with infinite barriers for the electrons (the same results given by models 1 and 2, respectively, in Fig. 2) are consistent with this experimental bound. From Fig. 2 we see that the result given by model 3 for infinite electron barriers is ≈ 1.25 psec. We have pointed out above that the macroscopic models are not appropriate for a quantitative treatment of the phonon contribution to the relaxation rates. The present results based on model 3 are close to the bound estimated in the experiment, and the comparison of these results with experiment suggests that additional physical effects may be necessary in order to obtain fully quantitative agreement with experiment. Such effects may include electron penetration into the barrier, which can make quantitative changes in the selection rules, or consideration of more sophisticated lattice-dynamical models than the simple-cubic nearest-neighbor model of Huang and Zhu.

Based on infrared bleaching experiments, Seilmeier *et al.*[3] have given an estimate of the intersubband relaxation time for a 50-Å GaAs quantum well at 300 K of the order of 10 psec. For this quantum-well width we obtain from model 3 in Fig. 2 in a value of ≈ 5.0 psec which is in reasonable accord with experiment. In this case it has been suggested that physical effects such as poor confinement of the electrons in the upper subband[4] or the combined effects of electron screening, intervalley transfer, and nonequilibrium phonons[17] may need to be include in addition to the effects of the confined phonons discussed here.

ACKNOWLEDGMENTS

This work was supported in part by a U.S. Office of Naval Research (ONR) contract (T.L.R.).

[1]M. C. Tatham, J. F. Ryan, and C. T. Foxon, Phys. Rev. Lett. **63**, 1637 (1989), and unpublished.
[2]D. Y. Oberli, D. R. Wake, M. V. Klein, J. Klem, T. Henderson, and H. Morkoç, Phys. Rev. Lett. **59**, 696 (1987).
[3]A. Seilmeier, H.-J. Huber, G. Abstreiter, G. Weimann, and W. Schlapp, Phys. Rev. Lett. **59**, 1345 (1987).
[4]J. K. Jain and S. Das Sarma, Phys. Rev. Lett. **62**, 2305 (1989).
[5]B. K. Ridley, Phys. Rev. B **39**, 5282 (1989).
[6]R. Fuchs and K. L. Kliewer, Phys. Rev. **140**, A2076 (1965).
[7]J. J. Licari and R. Evrard, Phys. Rev. B **15**, 2254 (1977).
[8]A. K. Sood, J. Menendez, M. Cardona, and K. Ploog, Phys. Rev. Lett. **54**, 2111 (1985).
[9]K. Huang and B. Zhu, Phys. Rev. B **38**, 2183 (1988).
[10]K. Huang and B. Zhu, Phys. Rev. B **38**, 13 377 (1988).
[11]M. V. Klein, IEEE J. Quantum Electron. **QE-22**, 1760 (1986).
[12]M. Cardona, in *Lectures on Surface Science*, edited by G. R. Castro and M. Cardona (Springer-Verlag, Berlin, 1987), pp. 2–27.
[13]S. Rudin and T. L. Reinecke, Phys. Rev. B **41**, 3017 (1990).
[14]R. Lassnig, Phys. Rev. B **30**, 7132 (1984).
[15]E. P. Pokatilov and S. I. Beril, Phys. Status Solidi B **110**, K75 (1982); **118**, 567 (1983).
[16]A. K. Sood, J. Menendez, M. Cardona, and K. Ploog, Phys. Rev. Lett. **54**, 2115 (1985).
[17]D. J. Newson and A. Kurobe, Appl. Phys. Lett. **53**, 2516 (1988).